

## Multi-terminal magnetotransport measurements over a tunable graphene p-n junction created by AFM-nanomachining

H. Schmidt, D. Smirnov, J. Rode, and R. J. Haug

Citation: *AIP Conference Proceedings* **1566**, 175 (2013); doi: 10.1063/1.4848342

View online: <https://doi.org/10.1063/1.4848342>

View Table of Contents: <http://aip.scitation.org/toc/apc/1566/1>

Published by the *American Institute of Physics*

---

### Articles you may be interested in

[Tunable graphene system with two decoupled monolayers](#)

*Applied Physics Letters* **93**, 172108 (2008); 10.1063/1.3012369

---

**AIP** | Conference Proceedings

Get **30% off** all  
print proceedings!

Enter Promotion Code **PDF30** at checkout



# Multi-terminal magnetotransport measurements over a tunable graphene p-n junction created by AFM-nanomachining

H. Schmidt, D. Smirnov, J. Rode and R. J. Haug

*Institut für Festkörperphysik, Leibniz Universität Hannover, Germany*

**Abstract.** An Atomic Force Microscope is used to alter one part of a single layer graphene sample locally. Transport experiments at low temperatures are then used to characterize the different parts independently with field effect and Hall measurements. It is shown, that the nanomachining leads to an effective doping in the altered area and therefore to a difference in the charge carrier density of  $\Delta n = 3.5 \cdot 10^{15} \text{m}^{-2}$  between the unchanged and changed part. These two parts can be tuned with a global backgate to form a junction of different polarity, i.e. a p-n junction.

**Keywords:** Graphene, AFM, bipolar

**PACS:** 72.80.Vp, 73.22.Pr

## Introduction

One of the unique properties of single layer graphene is its bandstructure with conduction and valence band touching at the charge neutrality point (CNP). In the vicinity of this CNP, it exhibits a linear behavior and a zero energy bandgap, which makes it possible to not only tune the density but also the type of charge carriers continuously from electrons to holes. Samples with regions of different densities and types of charge carriers allow to study edge channel transport in graphene [1] and electron-hole interference [2] or to use arrays of graphene p-n junctions as quantum Hall resistance standard [3]. While a global backgate is often used to tune the whole sample, different techniques including topgates [4] and also chemical doping [5] are used to achieve a local variation in the charge carrier density. Here we show the use of an Atomic Force Microscope (AFM) to alter the electronic properties in a defined region and introduce an effective doping to one part of the sample.

## Sample Preparation

The standard technique of exfoliation of natural graphite [6] is used to obtain high quality graphene samples on top of a silicon wafer covered with 330 nm of  $\text{SiO}_2$ . Using optical microscopy, a single layer graphene flake is identified [7].

Afterwards, one area (region II) of the sample is manipulated with an AFM using a diamond coated tip (Nanosensors DT-NCHR) as sketched in Figure 1. The tip is moved multiple times over the surface in contact mode with a velocity of  $v_{\text{tip}} = 10^{-6} \text{ms}^{-1}$  and a fixed

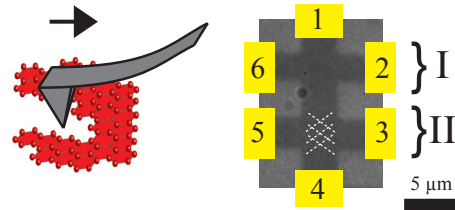


**FIGURE 1.** Left: Sketch of the nanomachining. The tip is moved over a single layer graphene sheet, introducing lattice defects. Right: Optical picture of the sample, divided into two parts, I and II. The latter is manipulated with the AFM as indicated by the white lines. The contacts are drawn in yellow.

force of  $F \approx 8 \mu\text{N}$ . Similar movements with the same parameters at the edge of the flake leave a well defined cut. In contrast to this, for the manipulation in the middle of the flake no changes are observed in the AFM picture taken afterwards. This has to be attributed to lower lattice energies at the edges or a self-healing process [8] of the lattice in the sample center.

After the nanomachining, the sample is structured into a Hallbar geometry and contacted by chromium gold leads, using standard electron beam lithography. Before the sample is measured, it is heated carefully for several hours to remove any residues from the fabrication process. An optical image of the contacted sample is shown in Figure 1 (right) with the changed (indicated by the dashed lines) and unchanged parts II and I. The sketched contacts are used to perform multi-terminal transport measurements.

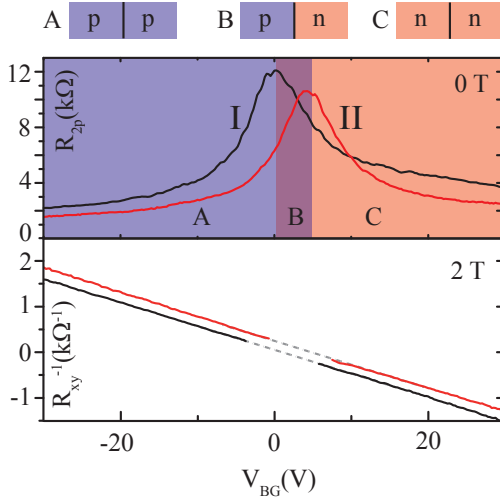


**FIGURE 2.** Top graph: Two terminal resistances of area I (black) and area II (red) as a function of backgate voltage. Above, the polarities of the two parts are sketched for the different voltage regimes. Bottom graph: Hall measurements of the two areas, performed at 2 Tesla.

## Transport Measurements

Transport measurements are performed in a Helium atmosphere at temperatures of down to 1.5 Kelvin. To characterize the two parts of the sample independently, AC-measurements with a current of  $100/\sqrt{2}$  nA are performed using contacts 2-6 (area I) and contacts 3-5 (area II), respectively. Figure 2 (top graph) shows the obtained resistances in the two parts as function of backgate voltage. In both cases the typical field effect with a maximum value at the CNP can be seen. Both curves exhibit a similar shape indicating similar mobilities in the order of  $10000 \text{ cm}^2 \text{ V}^{-1} \text{ s}^{-1}$ , taking into account the contact resistances and sample geometry. The position of the CNP in the altered part shows a clear shift to positive gate voltages of  $\Delta V = 5.3$  V, corresponding to a difference in charge carrier densities of  $\Delta n = 3.5 \cdot 10^{15} \text{ m}^{-2}$ .

To verify this shift also at higher voltages, four terminal Hall measurements are performed at 2 Tesla. The current is driven through contacts 1-4 and the Hall voltages according to the respective areas are measured. The resulting Hall resistances are shown in Figure 2 (bottom). Both Hall resistances are antiproportional to the backgate voltage and therefore to the charge carrier concentration as expected. While the slope is the same, excluding variation in the dielectric thickness, the whole curve is shifted. This confirms a constant difference in charge carrier concentration over the whole range of backgate voltages, being consistent with shift of the CNP as observed in the two terminal measurements.

This constant shift makes it possible to tune the system into different states as sketched in the top of Figure 2. For high backgate voltages, both parts exhibit electron or hole conductance with slightly different concentrations. Between 0.2 and 5.5 V, a p-n junction is created.

## Discussion

The transport measurements clearly show a local variation in charge carrier density due to the AFM nanomachining. An effect of cleaning and flattening of the graphene as reported in [9, 10] is unlikely, since the whole sample has been scanned several times and the doping level is enhanced and not reduced. Also, mobilities are similar in both areas. Contaminations on one part are also not likely, since both regions have been processed equally and carefully heated. After the measurements, the sample was taken out of the cryostat, heated and characterized again. While the positions of the CNPs in the two areas are only slightly shifted, the overall difference stays in the same order. Therefore, we attribute this stable effect to a change in the lattice of graphene, i.e. lattice defects introduced by the AFM. This method could be used to define more complicated samples with smaller doped regions, exhibiting interesting effects in transport, also at higher magnetic fields.

Our work is financial supported by the DFG Priority Program 1459 Graphene.

## REFERENCES

1. B. Özyilmaz et al., *Physical Review Letters* **99**, 166804 (2007).
2. D. Smirnov, H. Schmidt, and R. J. Haug, *Applied Physics Letters*, **100**, 203114 (2012).
3. M. Woszczyzna, M. Friedemann, T. Dziomba, Th. Weimann, and F. J. Ahlers, *Applied Physics Letters*, **99**, 022112 (2011).
4. J. R. Williams, L. DiCarlo, and C. M. Marcus, *Science* **317**, 638 (2007).
5. T. Lohmann, K. v. Klitzing, and J. H. Smet, *Nano Letters*, **9**, 1973 (2009).
6. K. S. Novoselov et al., *Science* **306**, 666 (2004).
7. P. Blake, E. W. Hill, A. H. Castro Neto, K. S. Novoselov, D. Jiang, R. Yang, T. J. Booth, and A. K. Geim, *Applied Physics Letters*, **91**, 063124 (2007).
8. R. Zan, Q. M. Ramasse, U. Bangert, and K. S. Novoselov, *Arxiv*: 1207.1487 (2012).
9. A. M. Goossens, V. E. Calado, A. Barreiro, K. Watanabe, T. Taniguchi, and L. M. K. Vandersypen, *Applied Physics Letters*, **100**, 073110 (2012).
10. N. Lindvall, A. Kalabukhov, and A. Yurgens, *J. Appl. Phys.*, **111**, 064904 (2012).